Journal of Cleaner Production 250 (2020) 119458

Contents lists available at ScienceDirect

Journal of Cleaner Production

journal homepage: www.elsevier.com/locate/jclepro

# Propionylation-modified chitin with improved solubility in green ethanol/water binary solvents for sustainable film and coating applications

Tuhua Zhong [a], Michael P. Wolcott [a], Hang Liu [a, b], Jinwu Wang [a, c, *]

[a] Composite Materials & Engineering Center, Washington State University, Pullman, WA, 99164, USA
[b] Department of Apparel, Merchandising, Design and Textiles, Washington State University, Pullman, WA, 99164, USA
[c] Forest Products Laboratory, U.S. Forest Service, Madison, WI, 53726, USA

ARTICLE INFO

*Article history:*
Received 29 July 2019
Received in revised form
20 November 2019
Accepted 24 November 2019
Available online 25 November 2019

Handling Editor: M.T. Moreira

*Keywords:*
Acylation
Chitin propionate
Ethanol/water binary solvent
Transparent films
Coatings

ABSTRACT

The use of less-toxic solvents is highly desirable for biopolymer processing and applications to meet sustainability while alleviating environmental burdens. In this study, chitin was propionylated to improve its solubility. The highly propionylated chitin exhibited considerably improved solubility (up to 96%) in a binary ethanol/water solution as compared to almost insolubility in a single solvent (either ethanol or water). Transparent films were prepared with acidified solutions and possessed excellent mechanical properties with a tensile strength up to 40 MPa and Young's modulus of 1.3 GPa. When the solution of the chitin propionate solution was employed as a coating on a paper substrate, the chitin propionate coating was found to improve the tensile strength of the paper from 64 MPa up to 84 MPa, and it also significantly decreased the surface energy to improve water resistance. These results suggest that chitin propionate that is dissoluble in ethanol/water binary solvents has potential use for new sustainable bio-based films and coatings in practical applications.

Published by Elsevier Ltd.

## 1. Introduction

Sustainable packaging materials based on polysaccharides or their derivatives have received much attention in recent years due to their renewability and biodegradability, which can help to alleviate land and ocean pollutions generated by petroleum-derived packaging products. Chitin is the second most abundant biopolymer on earth and commonly obtained from shrimp, lobster and crab shells which are produced at a rate of 6–8 million tonnes globally every year; these shells, containing 15–40% chitin, are often discarded as food waste from the canning industry (Kumar, 2000; Yan and Chen, 2015). Efficient use of this underutilized and abundant biopolymer can create more economic and environmental benefits. Chitin is biodegradable, which can be degraded and depolymerized by various enzymes such as chitinases, chitosanases, and non-specific enzymes like carbohydrases and proteases (Kaczmarek et al., 2019). Sustainable and biodegradable products based on chitin and chitin derivatives may be used as a potential replacement for petroleum-based products, thus benefiting the environment. However, chitin cannot dissolve in common organic solvents because of its supramolecular structure that formed by ample inter- and intramolecular hydrogen bonds, which makes it difficult in the processing and restricts its applications (Rinaudo, 2006). Although chitin can dissolve in a few solvents such as dimethylacetamide/lithium chloride (DMAc/LiCl), or ionic liquids, these solvents are either toxic or expensive, which make them impractical in industrial applications (Barber et al., 2013; Poirier and Charlet, 2002; Qin et al., 2010). The poor solubility of chitin is still the main barrier to its practical applications. The presence of a large number of hydroxyl groups in chitin offers a wide range of possibilities for its chemical modifications aiming at improving its solubility in common organic solvents, thereby leading to new chitin derivatives.

Acylation chemistry has been widely used in chemical modifications of cellulose, which produces a wide range of cellulose esters for coating additives and plastics (Edgar et al., 2001). Chitin has a similar structure to cellulose, but it has an acetamido group at the C2 position instead of a hydroxyl group in the pyranose ring (Kurita,

* Corresponding author. Forest Products Laboratory, 1 Gifford Pinchot Dr, Madison, WI 53726, USA.
*E-mail address:* jinwu.wang@usda.gov (J. Wang).

https://doi.org/10.1016/j.jclepro.2019.119458
0959-6526/Published by Elsevier Ltd.

1998). Well-developed acylation chemistry for cellulose could be adopted to modify chitin to yield chitin esters. Acylation enables the substitution of the hydrogen of hydroxyl groups of chitin with an acyl group to form less hydrophilic esters, which can weaken or break down the hydrogen bonds and thus leading to improvement in its solubility in organic solvents (Draczynski, 2011; Sugimoto et al., 2010; Van Luyen and Rossbach, 1995; Yang et al., 2009). Synthesis reactions may occur in a heterogeneous process or a homogeneous process. In the heterogeneous process, chitin may be treated with an organic acid anhydride and a catalyst (usually sulfuric acid or perchloric acid) in the absence of solvents. For example, Draczynski (2011) produced chitin acetate/butyrate by the heterogeneous process in which the mixture of two organic acid anhydride as acylation agents and perchloride acid as a catalyst in the presence of non-solvent for the starting chitin. The homogeneous process often requires the dissolution of chitin prior to the reaction with an organic acid anhydride or acyl chlorides. For example, Teramoto et al. (2006) produced different chitin esters under homogeneous conditions: chitin was first dissolved in DMAc/5%LiCl solution, subsequently, the acylation occurred with the addition of pyridine as a catalyst. To date, different chitin esters have been reported in the literature, but the information on the practical use of these chitin esters are still rare. It is well known that commercially available cellulose esters, cellulose acetate, cellulose propionate, cellulose acetate propionate, and cellulose acetate butyrate have been widely applied in coatings, additives, plastics, optical films, membranes, and composites, because cellulose esters can provide qualities such as good flow and leveling, inter-coat adhesion, sag resistance when applied as coating additives, meanwhile, cellulose ester films are optically clear, very tough and hard, and possess a high degree of ultraviolet stability (Edgar et al., 2001). Structurally similar to cellulose esters, chitin esters might also have great potential to be used in the coatings and plastic film packaging applications. In this research, we are searching for less-toxic organic solvents for processing chitin esters and exploring the applicability of chitin esters in film and coating applications.

There are some investigations on the solubility of chitin esters in organic solvents. For example, chitin acetate with a degree of acetyl substitution of 2 was found to be only soluble in acids such as formic acid (Van Luyen and Rossbach, 1995). Chitin propionate, chitin butyrate, chitin valerate, and chitin caproate were found to be soluble in DMAc, dimethylformamide (DMF), dimethyl sulfoxide (DMSO), acetone, and methanol (Sugimoto et al., 2010). Draczynski (2011) and Yang et al. (2009) produced chitin mixed ester films via the solution casting of chitin mixed esters in DMF followed by drying at room environment for 2∼3 days due to its high boiling point. Skołucka-Szary et al. (2016) also created some chitin hexanoate and chitin butyrate films by solution casting in acetone. However, in practical applications, especially in the food industry, it often demands low-toxic solvents such as ethanol. In addition, little attention has been paid to the use of ethanol/water binary solvents for chitin esters. The solubility of polymers in binary solvent systems is often unpredictable. Some binary solvents are found to improve the solubility of polymers, whereas these polymers are not able to dissolve in the individual ones (Hoogenboom et al., 2010; Zhang and Hoogenboom, 2015). For example, poly(methyl acrylate) (PMA) and poly(methyl methacrylate) (PMMA) polymers with ester groups were found not soluble in neither pure ethanol nor pure water, but soluble in ethanol containing a certain amount of water (Can et al., 2011; Hoogenboom et al., 2010; Zhang et al., 2012). To our knowledge, the solubility of chitin esters in the binary solvents with ethanol and water remains unstudied.

In the present work, we prepared chitin ester using propionic anhydride as an acylating agent and perchloride acid as a catalyst by the heterogeneous process to obtain highly substituted chitin propionate. This study aims to investigate the dissolution of chitin propionate in ethanol/water binary solvents with various ethanol concentrations. Subsequently, chitin propionate in aqueous ethanol solutions was employed in the transparent film preparation; in the meantime, it was also applied as a coating material on the paper substrate. We investigated microstructure, mechanical properties and surface energy of chitin propionate films. The surface morphology, mechanical properties and surface energy of chitin propionate coated paper were also determined.

## 2. Materials and methods

### 2.1. Materials

Chitin from shrimp shells (powder, practical grade), propionic anhydride (97%), perchloric acid (ACS reagent, 70%), diiodomethane (ReagentPlus, 99%), N,N-Dimethylacetamide (DMAc, anhydrous, 99.8%) were purchased from Sigma-Aldrich. Glacial acetic acid (ACS reagent) was purchased from EMD Millipore Corporation. Ammonium hydroxide was purchased from J.T. Baker. Glyceryl triacetate (GTA) was kindly provided by Siegwerk USA Co. Paper (Multipurpose paper, standard 92, recycled 100%) was from Georgia-Pacific. Ethanol (200 proof, anhydrous) was purchased from Decon Labs, Inc. Lithium chloride (LiCl, lab grade) was purchased from Fisher Science Education.

### 2.2. Synthesis of chitin propionate

A reaction mixture was prepared with the 1.0/6.6/0.5 wt ratio of chitin/propionic anhydride/perchloric acid. Twenty grams of the chitin power was used for each batch, around 12.3 wt% of the reaction mixture. Propionic anhydride and perchloric acid were precooled at $-4\,^{\circ}C$ for 1 h. Then, the perchloric acid was added dropwise into the propionic anhydride; subsequently, the chitin powder was added. The mixture was placed in a water/ice bath at $0\,^{\circ}C$ for the first 30 min and then at room temperature under stirring for 2.5 h. After the propionylation, the diluted acetic acid solution was added to the mixture to hydrolyze unreacted propionic anhydride. The product water-insoluble chitin propionate was separated from the mixture through water precipitation, then washed and repeatedly filtered until the pH was neutral, and finally dried in the oven at $70\,^{\circ}C$ for 24 h. The average weight of the obtained chitin propionate products was 26.3 g, and the yield was around 132%. The large yield was ascribed to the introduction of large propionyloxy groups in chitin propionate molecules.

### 2.3. Preparation of chitin propionate films

Chitin propionate films were prepared by solution casting of soluble chitin propionate in ethanol/water binary solvents. Three solutions were made from an aqueous mixture with an ethanol percentage at 90 wt%, 70 wt%, and 50 wt%, respectively, and the chitin propionate at a concentration of 1.8 wt% for all the solutions. Acidified solutions were prepared by acidifying the 90 wt% solution to pH 3.5 with acetic acid. Plasticized solutions were prepared by adding 40 or 60 wt% GTA plasticizer (based on the dry weight of the chitin propionate) to the acidified solution. Chitin propionate films were prepared by casting the solutions onto a leveled silicon mold (55 mm × 25 mm), dried overnight at room temperature in a fume hood, and then peeled off the mold. The acidified and plasticized solutions generated a series of transparent and plasticized chitin propionate films of 30∼40 μm in thickness; these samples were coded as neat CP, CP/GTA40, and CP/GTA60. All films were stored in a desiccator for 48 h before use and characterization.

### 2.4. Preparation of chitin propionate coated paper

The solution of chitin propionate, made in acidified 90% aqueous ethanol, was applied to the paper substrates with a wet thickness of 100 $\mu$m using a K101 Control Coater (RK Print Coat Instruments, UK). One side of the paper was coated, and the coating was dried at ambient conditions before the other side was coated. Based on the number of coating (one time and three times) on each side of the paper substrate, the samples were coded as CP(1) coated paper, and CP(3) coated paper, the paper substrate without chitin propionate coating was used as a control, coded as uncoated paper.

### 2.5. Fourier transform infrared spectroscopy (FTIR)

Fourier transform infrared spectra of chitin and chitin propionate were recorded using a Nicolet iS-50 FTIR spectrometer (Thermo Fisher Scientific, USA). The measurements were performed under the absorbance mode from 4000 $cm^{-1}$ to 400 $cm^{-1}$ with a 4 $cm^{-1}$ resolution and 64 scans.

### 2.6. $^1H$ nuclear magnetic resonance (NMR)

Liquid-state $^1H$ nuclear magnetic resonance (NMR) spectrum of the chitin propionate was measured at a scan number of 32 in the chemical shift range of 0–12 ppm by a Varian 400-NMR spectrometer (400 Hz, Bruker, USA). The chitin propionate was dissolved in deuterated dimethyl sulfoxide (DMSO-$d_6$). The degree of substitution of propionyl groups ($DS_{pr}$) and the degree of deacetylation (DD) was calculated using the following formulas [1] & [2] (Teramoto et al., 2006):

$$DS_{pr} = \frac{7I_{CH_3}}{3I_{H1-6}} \quad [1]$$

$$DD = 1 - \frac{7I_{Ac}}{3I_{H1-6}} \quad [2]$$

Where $I_{CH_3}$ is the integral area of the intensity of the signals of the methyl protons of propionyl groups, $I_{Ac}$ is the integral area of the intensity of the signals of the methyl protons of N-acetamido groups at the C2, $I_{H1-6}$ is the integral area of the intensity of the signals of seven protons of the anhydroglucose residue.

### 2.7. X-ray diffraction (XRD)

The diffractograms of the chitin and chitin propionate were recorded using a Miniflex 600 X-ray powder diffractometer (Rigaku, Japan) with a Cu Kα X-ray source ($\lambda = 0.1548$ nm) at 40 kV and 15 mA. Crystallinity index (CrI) was estimated using an empirical equation [3] as described by Fan et al. (2008) and Zhang et al. (2005).

$$CrI = \frac{(I_{110} - I_{amorphous})}{I_{110}} \times 100\% \quad [3]$$

where $I_{110}$ is the intensity of the diffraction peak (110) and $I_{amorphous}$ is the intensity of the amorphous part at $2\theta = 16.0°$.

### 2.8. Determination of soluble fraction of chitin propionate in ethanol/water solvent mixtures

The chitin propionate was dissolved in various ethanol/water solvent mixtures at room temperature for seven days. The undissolved portion of the chitin propionate was removed by centrifugation. The soluble fraction was calculated based on the following formula [4]:

$$\text{Soluble fraction} = \frac{Concentration_f}{Concentration_i} \times 100\% \quad [4]$$

Where $Concentration_i$ is the initial concentration of chitin propionate in ethanol/water solvent mixtures and $Concentration_f$ is the final concentration of chitin propionate solution after the removal of the undissolved chitin propionate. The concentration was determined by calculating the ratios of the weights before and after the drying chitin propionate solution at 70°C overnight.

### 2.9. Scanning electron microscopy (SEM)

The microstructure of chitin propionate films and the surface morphology of chitin propionate coated paper before and after the tensile test were observed with an SEM instrument (FEI Quanta 200F, FEI Company, USA) at 20 kV. All the samples were coated with platinum using the sputtering process before SEM observation.

### 2.10. Light transmittance measurement

The light transmittance of the acidified and plasticized chitin propionate films was measured from 200 nm to 700 nm with a Lambda-25 UV–Vis spectrophotometer (PerkinElmer, USA).

### 2.11. Mechanical properties test

The tensile strength of chitin propionate films and chitin propionate coated paper was measured by an Instron 4466 testing system (Instron Co., USA) equipped with a 5 kN load cell. The initial grip separation length was 2 mm, and the testing speed was 2 mm/min. Five specimens for each sample were measured.

### 2.12. Dynamic mechanical analysis (DMA)

The dynamical mechanical properties of the plasticized films in tension were measured with a DMA instrument (Q800, TA Instruments) under the strain amplitude of 25 $\mu$m and preload force of 0.001N, ramping from 30 °C– 200 °C at 3 °C /min.

### 2.13. Contact angles and surface energy measurement

The contact angle of the plasticized chitin propionate films and chitin propionate coated paper was measured by the sessile drop technique (VCA Optima Video Contact Angle System, AST Products Co., USA). The measurements were performed at room temperature with a polar liquid (water) and an apolar liquid (diiodomethane). The surface energy was calculated using Geometric-Mean method based on the two contact angles with SE-2500 surface energy (dyn/cm) calculation software (AST Products Co., USA).

### 2.14. Intrinsic viscosity measurement and molecular weight determination

The intrinsic viscosity [η] was measured by capillary solution viscometry. Chitin and propionylated chitin were dissolved in N, N-dimethyl acetamide/5% lithium chloride (DMAc/5%LiCl) at three different concentrations: 0.02, 0.04, and 0.06 g/dL for the chitin, 0.32, 0.64, and 0.96 g/dL for the propionylated chitin. The viscosity of each concentration was determined with a calibrated Ubbelohde viscometer (Cannon, USA) in a water bath with a controlled temperature of 25±0.1°C. The flow time for each concentration was measured five times. To evaluate the intrinsic viscosity, the data of reduced viscosity $\eta_{red}$ was first calculated using the equation [5]:

$$\eta_{red} = \frac{\frac{t_i}{t_0} - 1}{c} \quad [5]$$

where $t_i$ is the flow time of chitin or propionylated chitin solutions in DMAc/5% LiCl, $t_0$ is the flow time of solvents, $c$ is the chitin or propionylated chitin concentration (Czechowska-Biskup et al., 2018). Subsequently, the reduced viscosities were plotted in one graph as a function of concentration c, the [η] was the value of intercept of the fitted straight lines with the ordinated axis as a result of the extrapolation of the concentration to zero. The molecular weight ($M_v$) was determined according to the Mark-Houwink equation [6]:

$$[\eta] = kM_v^a \quad [6]$$

The $k$ value is 2.1 $\times 10^{-4}$ and $a$ value is 0.88 for the give solution system, temperature and chitin materials (Min et al., 2004).

## 3. Results and discussion

### 3.1. Characteristics of chitin propionate

The scheme of the propionylation of chitin is shown in Fig. S1. The chitin propionate was manufactured by a heterogeneous process in which chitin was treated by acylating agent propionic anhydride and perchloride acid as catalyst in the presence of non-solvents. The conversion of hydroxy groups into acyloxy groups in chitin is confirmed by the comparison of the FTIR spectra of starting material chitin and propionylated chitin (Fig. 1a). The FTIR spectrum of the chitin shows its characteristic amide bands around 1662 $cm^{-1}$ and 1558 $cm^{-1}$, which corresponded to the stretching of C═O in the amide I and the overlapping of the C–N stretching and N–H bending in the amide II, respectively (Cárdenas et al., 2004; Rinaudo, 2006). The two bands around 1740 $cm^{-1}$ and 1180 $cm^{-1}$ in the FTIR spectrum of the chitin propionate were attributed to the C═O stretching and C–O stretching of esters, which were the characteristic bands of fatty acid esters (Szosland, 1996). The intensity of the band of O–H stretching around 3425 $cm^{-1}$ was lower than that of the chitin, which further suggests that hydrogen atoms of hydroxyl groups were replaced by propionyl moieties, a shoulder band was observed at around 3500 $cm^{-1}$ might be ascribed to O–H stretching that was induced primarily by water molecules.

As can be seen from Fig. 1b, the $^1$H NMR spectrum confirmed the substitution of propionyl moieties for hydrogen atoms of hydroxyl groups in the propionylated chitin. The signals around 3.44 ppm ~ 4.91 ppm represent 7 protons at the C1–C6 positions of anhydro-N-acetylglucosamine and/or anhydro-N-glucosamine units, and the integral area of these signals was normalized as 7.00 for 7H as the reference signal to which other signals were scaled. Two signals around 0.94 ppm and 1.04 ppm were assigned to methyl protons (-$CH_3$) of propionyl groups at two different positions of the pyranose ring, which had total integral area of 6.00. The other two signals around 2.11 ppm and 2.32 ppm correspond to methylene protons (-$CH_2$) of propionyl moieties at the two different positions, which had total integral area of 3.98. The signal at 1.66 ppm was attributed to the methyl protons (-$CH_3$) of acetamido groups (-NHAc). Another signal around 7.70 ppm was assigned to the amino proton (–NH–) of acetamido groups. Two signals around 2.47 ppm and 3.18 ppm were attributed to the protons from DMSO and $H_2O$ in DMSO, respectively. The ratio of the integral areas of 7.00:3.98:6.00 as shown in Fig. 1b almost equals to 7:4:6. The 4:6 ratio has been expected since there are two methylene protons and three methyl protons in each propionyl group. There are 7 protons at the C1–C6 positions per repeat anhydro-N-acetylglucosamine or anhydro-N-glucosamine unit of chitin. Thus, the 7:4:6 ratio indicates that almost all the hydroxyl groups were substituted with propionyl groups at the C3 and C6 positions. The calculated acetyl content at the C2 position in the chitin propionate was approximate 0.93 per repeat anhydro-N-acetylglucosamine or anhydro-N-glucosamine unit; the theoretical value should be 1.0 if deacetylation did not occur indicating the presence of a few amino groups, i.e., the degree of deacetylation (DD) of 0.07 in the chitin propionate. The amino groups in the chitin propionate might mainly

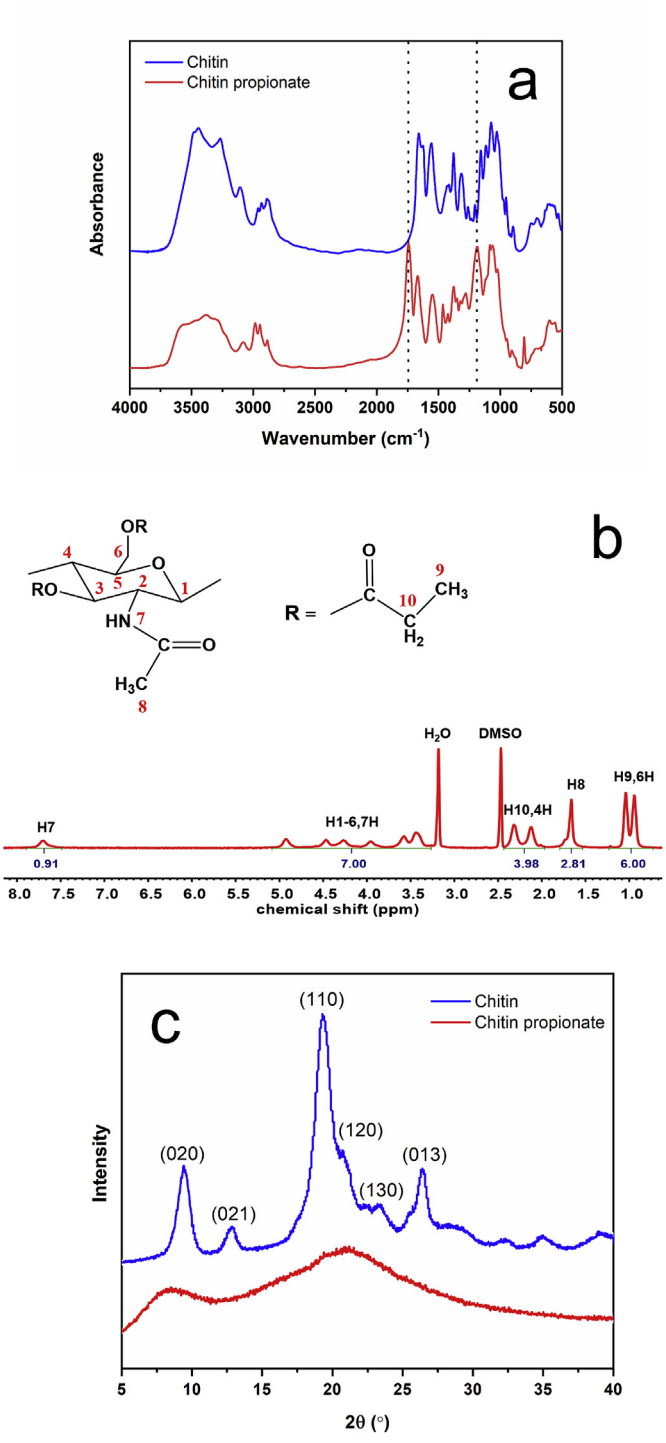


**Fig. 1.** (a) FTIR spectra of chitin and chitin propionate; (b) $^1$H NMR spectrum of chitin propionate in deuterated DMSO-$d_6$; (c) XRD patterns of chitin and chitin propionate.

inherit from the raw chitin because small partial deacetylation often occurs during extraction, and often resulting in approximate 5–15% amino groups in raw chitin (Cárdenas et al., 2004; Pillai et al., 2009; Teramoto et al., 2006). The obvious peak signals for methylene protons and methyl protons of the resulting amide should be yielded in the $^1$H NMR spectrum if the propionyl substitution occurred with the free amino groups at C2 position, but such peaks were not evidently observed, indicating negligible or no propionylation occurred at C2−$NH_2$ position. Teramoto et al. (2006) and Yang et al. (2009) also reported that little (negligible) or no propionylation occurred at C2−$NH_2$.

The crystalline structure of chitin was dramatically altered after the propionylation, as indicated by the diffractograms in Fig. 1c. The original chitin had a typical crystalline structure of α-chitin with the six characteristic peaks at $2\theta = 9.4°$, 12.6°, 19.4°, 20.5°, 23.5°, and 26.3°, corresponding to the (020), (021), (110), (120), (130) and (131) crystallographic planes, respectively (Duan et al., 2013). Based on the calculation from the intensity of the (110) crystallographic plane and the intensity of amorphous chitin at $2\theta = 16°$, the CrI of the chitin powder was 90% (Fan et al., 2008; Zhang et al., 2005). After the propionylation, the peak intensity of the characteristic crystallographic planes significantly decreased or even disappeared, as shown in Fig. 1c, the broadening of the remaining reflections indicated an amorphous structure of the polymer (Binias et al., 2005). As shown in Fig. S2, the intrinsic viscosity of the raw chitin was 14.52 dL/g, and the molecular weight was estimated with the Mark-Houwink equation to be around 310 kDa. The intrinsic viscosity of the propionylated chitin was 0.98 dL/g. The molecular weight of the propionylated chitin cannot be estimated from the Mark-Houwink equation directly in this study since the Mark-Houwink coefficients for the propionylated chitin are not available. The great reduction in the intrinsic viscosity and disappearance of peaks in the diffractogram indicate that the propionylation not only damaged the crystal structure but also might have degraded chitin chains, thus resulted in a much lower intrinsic viscosity.

### 3.2. The soluble fraction of chitin propionate in ethanol/water binary solvents

Ethanol with a certain amount of water exhibits strong solvating capability for chitin propionate. As shown in Fig. 2a, the chitin propionate is almost insoluble in either pure ethanol or pure water. Upon admixing of ethanol with a small amount of water (5 wt%), the soluble fraction of the chitin propionate in the solvent mixture was dramatically increased up to 69%. With increasing the water content to 10 wt% in the binary solvent, the soluble fraction was brought up to around 93%. The maximum solubility of chitin propionate was around 96% in the binary solvent containing 30 wt% water. As mentioned previously, polymers such as PMA and PMMA with ester groups exhibited similar dissolution behavior in the ethanol/water binary solvents. The mechanism behind this interesting solubility behavior of these polymer esters in binary ethanol/water mixtures has not fully understood yet. One explanation is that the formation of hydration shells around carbonyl groups of polymer side ester moieties and the interaction of the ensuing hydration shells with ethanol molecules via hydrogen bonding result in solubility maxima for some polymer esters in the binary ethanol/water mixture (Can et al., 2011; Hoogenboom et al. 2008, 2009, 2010; Zhang and Hoogenboom, 2015). Hoogenboom et al. (2009) have confirmed this hypothesis by small-angle neutron scattering, indicating the presence of a single deuterated water molecule per PMMA repeat unit. Similar phenomenon for solubility maxima of chitin propionate bearing ester moieties in ethanol/water might be also ascribed to the presence of such hydration shell

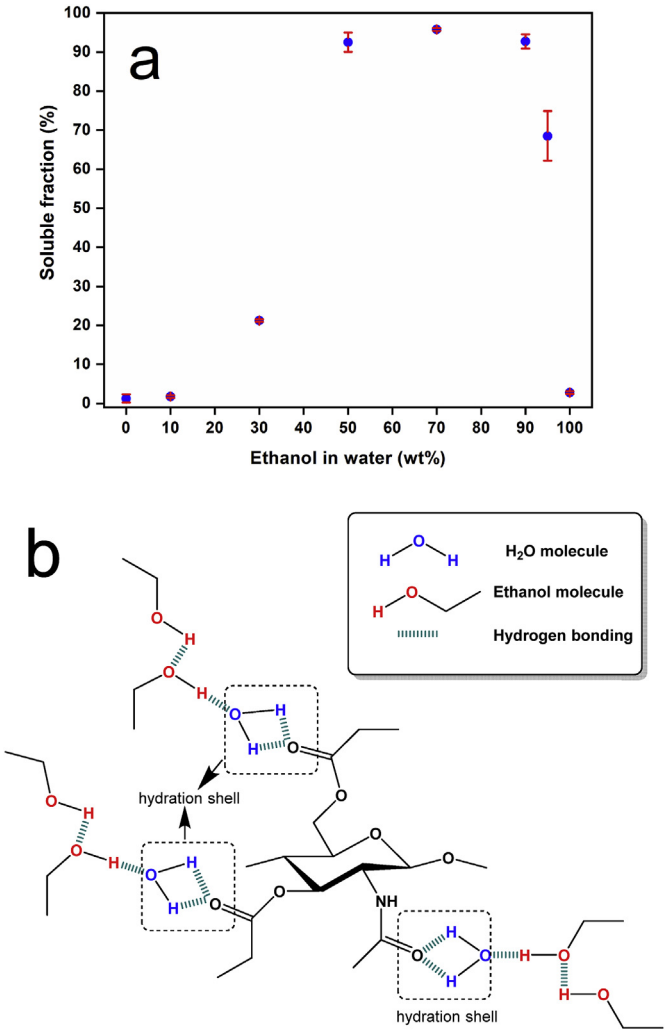


**Fig. 2.** (a) Soluble fraction of chitin propionate in ethanol/water binary solvents with various ethanol concentrations; (b) schematic representation of potential hydrogen bonding among chitin propionate repeat unit, water molecules, and ethanol molecules.

around carbonyl groups of chitin propionate that can further interact with ethanol molecules via hydrogen bonding, thus enhancing solubility in this particular binary ethanol/water mixture, as schematically depicted in Fig. 2b (Hoogenboom et al., 2009, 2010). However, a systematic investigation in future work is still needed to fully elucidate the mechanism behind the solubility maxima of this specific chitin propionate in binary ethanol/water mixture but insoluble in pure water or in pure ethanol.

The solubility maximum occurred in the binary solvent containing 30 wt% water, that might be partly attributed to the possible presence of the most single, non-clustered water molecules in this specific ethanol solvent composition, which led to favorable hydrogen bonding between water and ester groups of chitin propionate (Can et al., 2011; Hoogenboom et al., 2008). Water clusters that dominantly exist in pure water can be broken down into dispersed monomers, water-dimers, trimers, and tetramers upon with the addition of a certain amount of ethanol (Hoogenboom et al., 2010; Noskov et al., 2005). With the water content over 50 wt% or lower than 10 wt% in the binary solvent, the soluble fraction decreased. It may due to the formation of more bulk water clusters in higher water content or less efficiency of hydration of polymers in lower water content, thus resulting in the lower solubility. As shown in Fig. 2a, when the solvent mixture contained

70 wt% water, the soluble fraction dramatically dropped to 21%, and the chitin propionate was almost insoluble in the solvent mixture with 90 wt% water.

### 3.3. Characteristics of chitin propionate films

The water content in the ethanol/water binary solvent affected the microstructure of the cast chitin propionate films after the removal of all the solvents. As can be seen from the inset photograph in Fig. 3a, the film prepared from the 90% ethanol solution exhibits the translucency. The SEM image of the fractured cross-section of the film reveals a porous microstructure (Fig. 3a), which caused light scattering, thus resulting in translucency. With increasing the water fraction, more irregular microstructures, including lamellae, microspheres, and pores (Fig. 3b) were formed in the cast film leading to an increased opaqueness. Up to the water fraction of 50%, the integral film could not be obtained and peeled off from the mold after the solvent evaporation (Fig. 3c). This system and process are akin to the phase inversion process for porous membrane preparation. The ethanol concentration in the binary solvent was below the azeotropic point, and ethanol was expected to evaporate out of the solution at a faster rate than water, causing the composition to have a higher water and chitin propionate content. The polymer eventually precipitated and formed a porous film (Wang and Padua, 2010).

Given that high water content in the binary solvent would result in lower drying speed in addition to the increased difficulty in forming an integral film, chitin propionate dissolving in the binary solvent containing only 10 wt% water was selected for further investigation to enhance its transparency. As illustrated in the inset photograph in Fig. 3d, the addition of acetic acid into chitin propionate in the binary solvent was found to reduce the porosity of the cast film and improve the transparency. A small number of amino groups existed in the chitin propionate structure, which was evidenced by DD value (approximate 0.07) in earlier $^{1}$H NMR analysis. The addition of acetic acid would result in the protonation of amino groups (-$NH_2$) into $-NH_3^+$, leading to the electrostatic repulsion among the chains of chitin propionate molecules; the protonation (ionization) might help further enhance the solubility of chitin propionate in ethanol/water mixture. The higher acidic water content in the composition in the last stage of the cast solution evaporation help reduce the formation of pores. It is analogous to the reason that the densification of cellulose nanofibril films upon drying from water, which was the combination of the capillary pressure of the evaporating solvent and the disruption of the hydrogen bonding network at the intersections of the particles by the solvent (Toivonen et al., 2018). When the solution was not acidified, the hydrogen bonding network among amino and

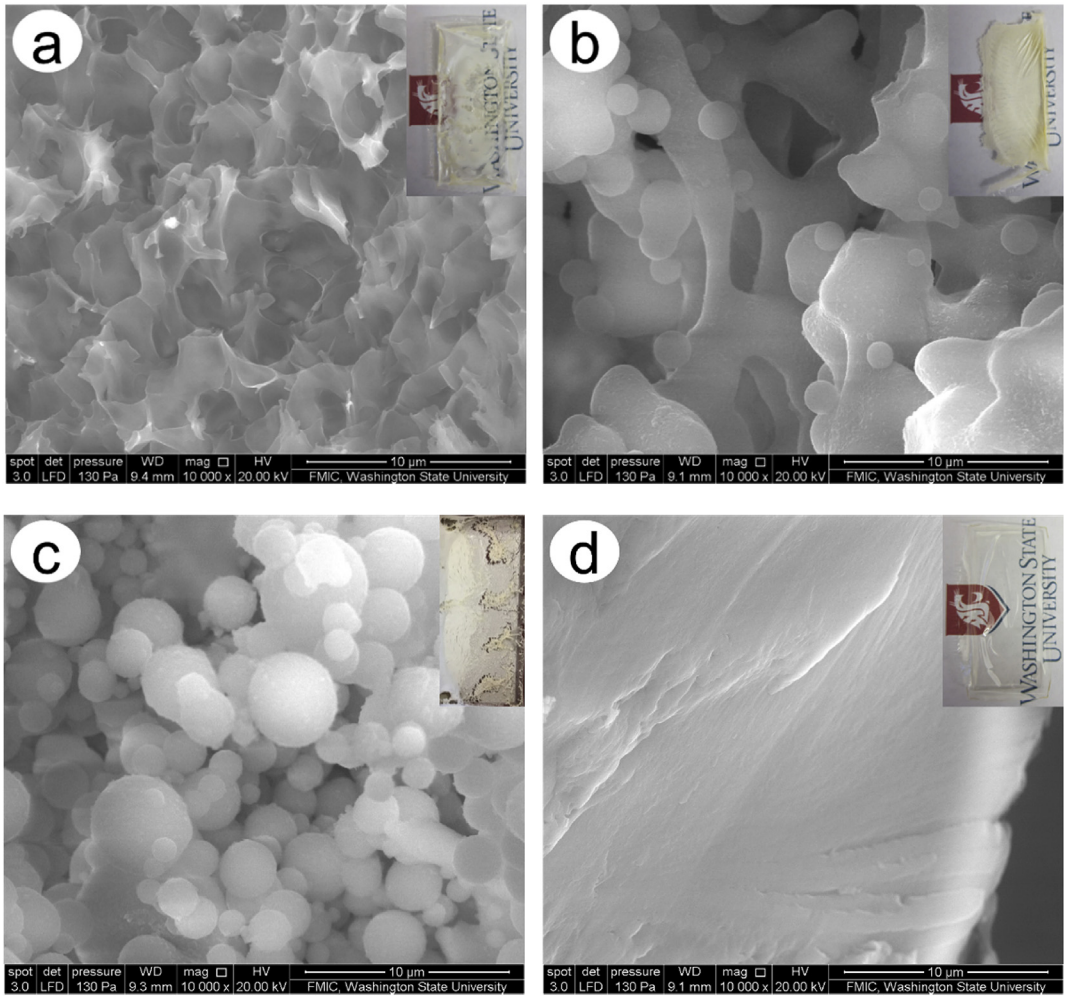


**Fig. 3.** SEM images of fracture cross-section of chitin propionate films from various solvent mixtures: (a) 90/10 %w/w ethanol/water; (b) 70/30 %w/w ethanol/water; (c) 50/50 %w/w ethanol/water; (d) 90 wt% aqueous ethanol acidified with acetic acid (pH = 3.5). Inset: photographs of the corresponding films.

carbonyl groups was no longer disrupted and could be considered physically crosslinked keeping pores from collapsing by the capillary pressure (Toivonen et al., 2018).

As displayed in Fig. 4a, the light transmittance of this chitin propionate film from the acidified solution was up to 92% in the visible light spectrum of 500 nm – 700 nm. The addition of GTA plasticizer did not compromise the transparency of chitin propionate films. The light transmittance decreased with the decreasing wavelength of the light in the UV region, indicating that the films blocked certain parts of UV lights, and more effectiveness of blocking UV lights at shorter wavelength was observed. Fig. 4b displays the typical stress-strain curves of the neat chitin propionate film and the plasticized ones, and the data of mechanical properties are summarized in Table 1. The tensile strength of the neat chitin propionate film was 40 MPa, but the elongation at break was only 4%, indicating its intrinsic brittleness. Plasticizer GTA improved the flexibility of the films because the low molecular weight GTA could be embedded in between chitin propionate molecule chains (Li et al., 2017). The elongation at break of the cast film was brought up to 17% and 25% after the addition of plasticizer GTA at 40 wt% and 60 wt%. However, the incorporation of plasticizer resulted in decreased tensile strength and Young's modulus, as shown in Table 1.

Fig. 4c shows the temperature dependence of storage modulus and tan $\delta$ of the neat chitin propionate film and the plasticized chitin propionate films. The chitin propionate films with plasticizer had lower storage modulus than the neat film with the temperature ranging from 30 $^{\circ}C$ to 150 $^{\circ}C$. This can be ascribed to the increased segmental motion in the chitin propionate backbone due to the incorporation of low molecular weight plasticizer, thereby decreasing the storage modulus (Park et al., 2004). The storage modulus of neat chitin propionate film decreased smoothly with increasing the temperature and exhibited glassy modulus up to the temperature around 150 $^{\circ}C$. Beyond the temperature of 150 $^{\circ}C$, the storage modulus began to decrease dramatically, indicating the transition from glassy state to a rubbery state. Another sudden drop in the storage modulus occurred around 190 $^{\circ}C$, suggesting that the film began to decompose; it appears that the film had no resistance to the temperature close to 190 $^{\circ}C$. It is interesting to note that there was a weak but broad tan $\delta$ peak in either CP/GTA40 film or CP/GTA60 film at the lower temperature around 80 $^{\circ}C$, which can be denoted as "secondary relaxation". Such broad peaks in the curve might be ascribed to a specific type of polymer-plasticizer interaction (Bao et al., 2015). The interaction between propionyl moieties of chitin propionate and acetyl moieties of glyceryl triacetate via hydrogen bonding and the easier rotation of chitin propionate molecular chain might be in part account for the occurrence of this tan $\delta$ peak. With increasing the plasticizer GTA content in the chitin propionate matrix, tan $\delta$ peak related to secondary relaxation became slightly broader.

### 3.4. Characteristics of chitin propionate coated paper

Chitin propionate as a coating on a paper substrate could alter the microstructure and mechanical properties of the paper substrate. As shown in Fig. 5a, the uncoated paper substrate exhibits a heterogeneous and rough surface due to the interlacement of cellulose fibers. With one layer coating, chitin propionate filled the interfibrillar cellulose fiber spaces, and the paper exhibits a relatively smooth surface. However, the interlacement of cellulose fibers and a few pores are still clearly observed in Fig. 5c. Repetitive coating three times on the paper substrate produced a smoother and more homogenous surface because more total solids were deposited on the paper surface, thus leading to the completely covered and filled pores of the paper substrates, as observed in

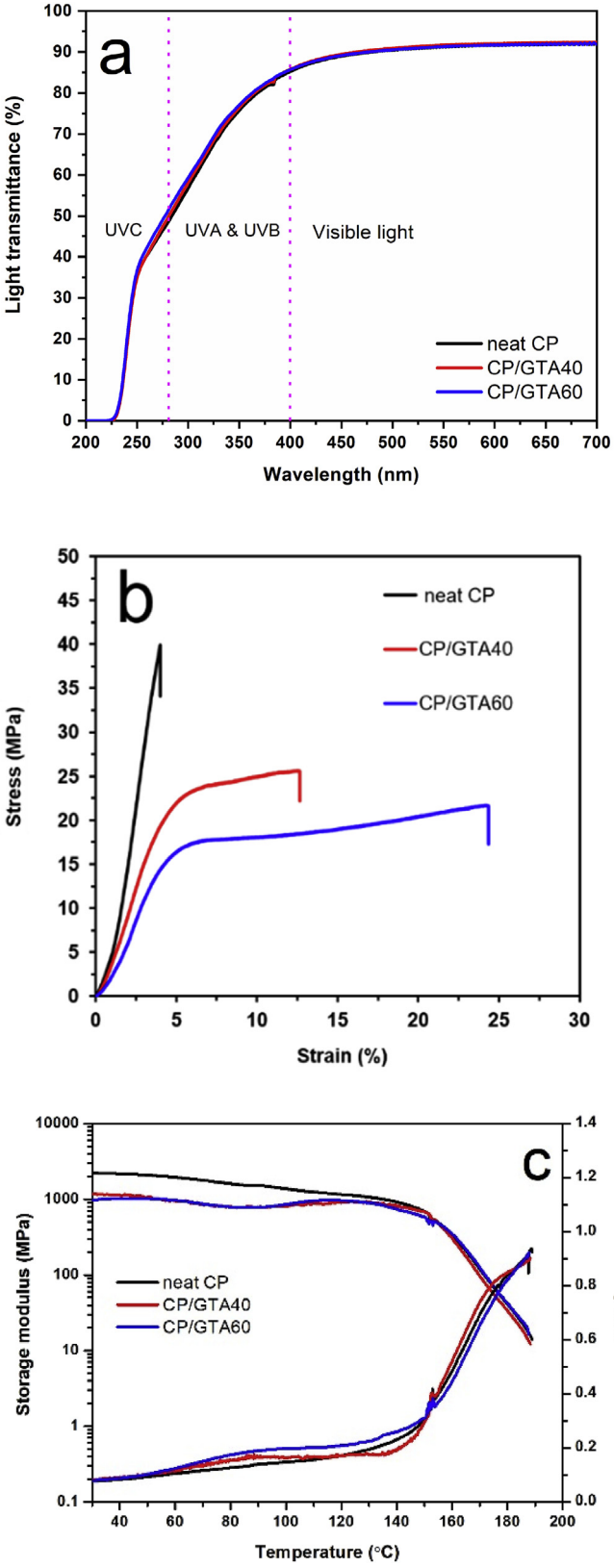


**Fig. 4.** (a) UV–Vis spectra; (b) typical stress-strain curves; (c) the temperature dependence of storage modulus and tan $\delta$ of the neat chitin propionate film and plasticized films.

**Table 1**
Summary of the mechanical properties of the neat chitin propionate and the plasticized chitin propionate films.

| Sample | Tensile strength at break (MPa) | Young's modulus (GPa) | Elongation at break (%) |
|---|---|---|---|
| neat CP | 40±3 | 1.3±0.1 | 4.3±0.2 |
| CP/GTA40 | 24±3 | 0.54±0.1 | 17±4 |
| CP/GTA60 | 21±3 | 0.48±0.1 | 25±1 |

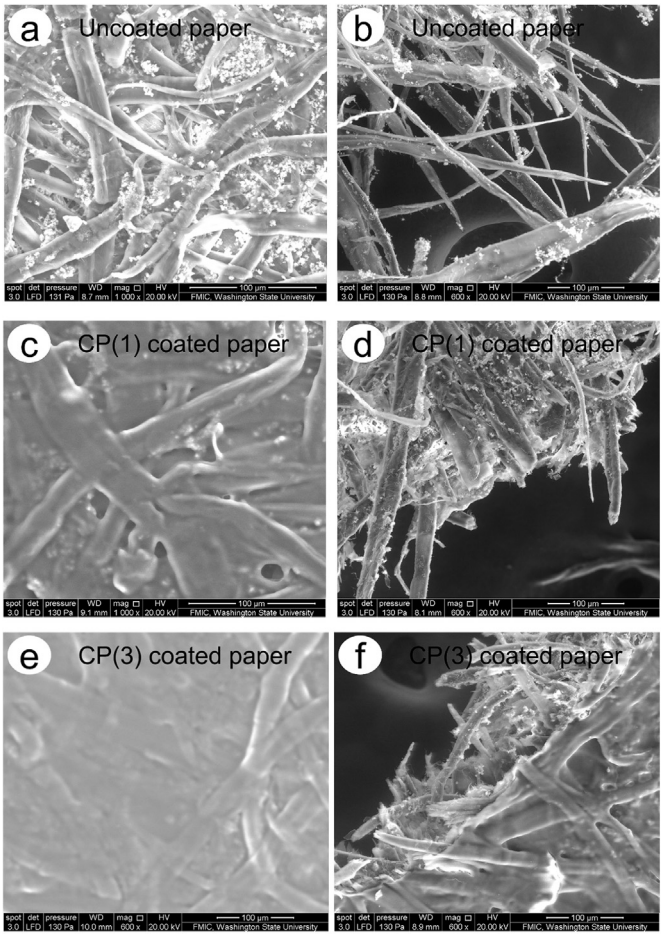


**Fig. 5.** Surface morphologies of the uncoated paper and chitin propionate coated paper before the tensile test (a, c, e) and fractured surfaces after the tensile test (b, d, f).

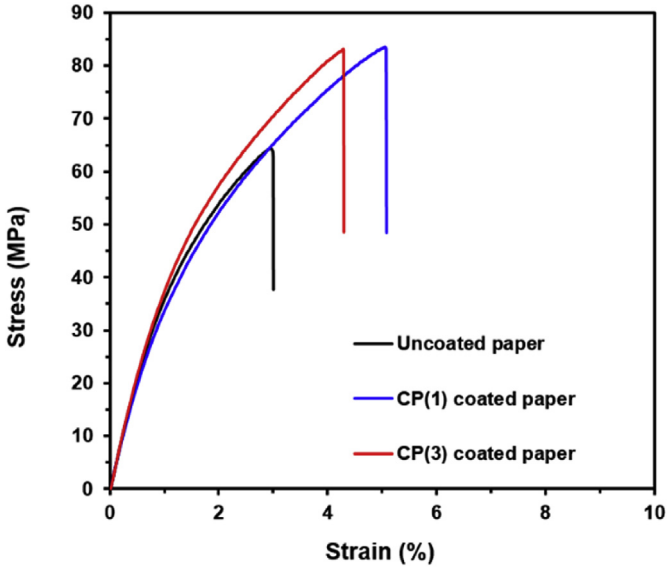


**Fig. 6.** Typical stress-strain curves of the uncoated paper and chitin propionate coated paper.

Fig. 5e.

As shown in Fig. 6, the tensile strength of CP(1) coated paper was brought up to 83.0 MPa from 64.4 MPa of the uncoated paper. Repetitive coating three times on the paper substrate only slightly increased the tensile strength to 83.6 MPa. It appears that one-time chitin propionate coating is sufficient to enhance the tensile strength. The improvement in the tensile strength of chitin propionate coated paper may be mainly attributed to that the chitin propionate was filled into the pores or spaces among the cellulose fibers to enhance the bonding among cellulose fibers. Fig. 5b reveals that after the tensile strength test, individual cellulose fibers were pulled out and separated from the uncoated paper substrate, whereas the cellulose fibers were still bonded together (Fig. 5d–f) after the tensile test for the coated paper. It accounts for why chitin propionate coatings could provide a significant improvement on the tensile strength of the paper substrate.

As can be seen from Table 2, the neat chitin propionate film exhibited a water contact angle of approximate 75°, whereas that of the plasticized films was around 69°. It might be ascribed to the presence of more hydrophilic plasticizer GTA on the surface of the plasticizer films, which may account for a slight increase in the surface energy of the plasticizer films. The uncoated paper exhibited a considerably low water contact angle (approximate 39°) and high surface energy (approximate 62 dyn/cm) because there were a large number of hydrophilic hydroxyl groups on the surface of cellulose fibers for uncoated paper. The increased water contact angle and decreased surface energy indicated that chitin propionate coatings could help to improve the water-resistance of paper substrates.

## 4. Conclusions

This work demonstrates the enhanced solubility of highly substituted chitin propionate in ethanol/water binary solvents. The dissolution of chitin propionate in less-toxic ethanol/water solvent mixtures might open its potential to be used in practical applications such as films, inks, and coatings. Highly transparent and plasticized chitin propionate films were successfully obtained with good tensile strength through acidified solution casting. Specifically, the neat chitin propionate films exhibited a tensile strength of 40 MPa and moderate surface energy of 39 dyn/cm. Plasticizer glyceryl triacetate was found to improve the flexibility of chitin propionate films, and the 60 wt% plasticizer loading increased the elongation at break from 4% to 25%. In this work, chitin propionate coating on a paper substrate was also demonstrated to provide improvement in the tensile strength from 63 MPa to 84 MPa, in the meanwhile, it could decrease the surface energy to improve the water-resistance of the paper substrate. Such performance of transparent films and coatings might open up many opportunities for this new sustainable bio-based material in packaging applications.

**Table 2**
Contact angles and surface energy of chitin propionate films and chitin propionate coated paper sheets.

| Samples | Water (°) | Diiodomethane (°) | Surface energy (dyn/cm) |
|---|---|---|---|
| neat CP | 75±4 | 46±2 | 39 |
| CP/GTA40 | 70±4 | 45±2 | 41 |
| CP/GTA60 | 69±2 | 47±3 | 40 |
| Uncoated paper | 39±3 | 23±4 | 62 |
| CP(1) coated paper | 62±4 | 38±2 | 47 |
| CP(3) coated paper | 61±2 | 39±2 | 47 |

Contact angle values recorded at the 60th second.

## Author contributions

Use this form to specify the contribution of each author of your manuscript. A distinction is made between five types of contributions: Conceived and designed the analysis; Collected the data; Contributed data or analysis tools; Performed the analysis; Wrote the paper.

For each author of your manuscript, please indicate the types of contributions the author has made. An author may have made more than one type of contribution. Optionally, for each contribution type, you may specify the contribution of an author in more detail by providing a one-sentence statement in which the contribution is summarized. In the case of an author who contributed to performing the analysis, the author's contribution for instance could be specified in more detail as 'Performed the computer simulations', 'Performed the statistical analysis', or 'Performed the text mining analysis'.

If an author has made a contribution that is not covered by the five pre-defined contribution types, then please choose 'Other contribution' and provide a one-sentence statement summarizing the author's contribution.

Tuhua Zhong: Conceived and designed the experiment and analysis, Collected the data, Contributed data, Performed the material properties chracterizations and data analysis, Wrote the paper. Michael Wolcott: Conceived and designed the experiment and analysis, Contributed analysis tools, Hang Liu: Conceived and designed the experiment and analysis, Contributed analysis tools, Revised the paper. Jinwu Wang: Conceived and designed the experiment and analysis, Performed the data analysis, Wrote and revised the paper.

## Declaration of competing interest

The authors declare that they have no known competing financial interests or personal relationships that could have appeared to influence the work reported in this paper.

## Acknowledgements

This work was supported by the Center for Bioplastics and Biocomposites (CB2), a National Science Foundation Industry/University Cooperative Research Center (Awards IIP-1439732 & 1738669).

## Appendix A. Supplementary data

Supplementary data to this article can be found online at https://doi.org/10.1016/j.jclepro.2019.119458.

## References

Bao, C.Y., Long, D.R., Vergelati, C., 2015. Miscibility and dynamical properties of cellulose acetate/plasticizer systems. Carbohydr. Polym. 116, 95–102.
Barber, P.S., Griggs, C.S., Bonner, J.R., Rogers, R.D., 2013. Electrospinning of chitin nanofibers directly from an ionic liquid extract of shrimp shells. Green Chem. 15 (3), 601–607.
Binias, D., Borinyec, S., Binias, W., 2005. Studies of the structure of polysaccharides in the process of alkaline treatment of dibutyrylchitin fibres. Fibres Text. East. Eur. 13 (5), 137–140.
Can, A., Hoeppener, S., Guillet, P., Gohy, J.F., Hoogenboom, R., Schubert, U.S., 2011. Upper critical solution temperature switchable micelles based on polystyrene-block-poly (methyl acrylate) block copolymers. J. Polym. Sci. Part A Polym. Chem 49 (17), 3681–3687.
Cárdenas, G., Cabrera, G., Taboada, E., Miranda, S.P., 2004. Chitin characterization by SEM, FTIR, XRD, and 13C cross polarization/mass angle spinning NMR. J. Appl. Polym. Sci. 93 (4), 1876–1885.
Czechowska-Biskup, R., Wach, R.A., Rosiak, J.M., Ulański, P., 2018. Procedure for determination of the molecular weight of chitosan by viscometry. Prog. Chem. Appl. Chitin Deriv. 23, 45–54.
Draczynski, Z., 2011. Synthesis and solubility properties of chitin acetate/butyrate copolymers. J. Appl. Polym. Sci. 122 (1), 175–182.
Duan, B., Chang, C., Ding, B., Cai, J., Xu, M., Feng, S., Ren, J., Shi, X., Du, Y., Zhang, L., 2013. High strength films with gas-barrier fabricated from chitin solution dissolved at low temperature. J. Mater. Chem. 1 (5), 1867–1874.
Edgar, K.J., Buchanan, C.M., Debenham, J.S., Rundquist, P.A., Seiler, B.D., Shelton, M.C., Tindall, D., 2001. Advances in cellulose ester performance and application. Prog. Polym. Sci. 26 (9), 1605–1688.
Fan, Y., Saito, T., Isogai, A., 2008. Chitin nanocrystals prepared by TEMPO-mediated oxidation of α-chitin. Biomacromolecules 9 (1), 192–198.
Hoogenboom, R., Becer, C.R., Guerrero-Sanchez, C., Hoeppener, S., Schubert, U.S., 2010. Solubility and thermoresponsiveness of PMMA in alcohol-water solvent mixtures. Aust. J. Chem. 63 (8), 1173–1178.
Hoogenboom, R., Rogers, S., Can, A., Becer, C.R., Guerrero-Sanchez, C., Wouters, D., Hoeppener, S., Schubert, U.S., 2009. Self-assembly of double hydrophobic block copolymers in water–ethanol mixtures: from micelles to thermoresponsive micellar gels. Chem. Commun. 37, 5582–5584.
Hoogenboom, R., Thijs, H.M., Wouters, D., Hoeppener, S., Schubert, U.S., 2008. Tuning solution polymer properties by binary water–ethanol solvent mixtures. Soft Matter 4 (1), 103–107.
Kaczmarek, M.B., Struszczyk-Swita, K., Li, X., Szczesna-Antczak, M., Daroch, M., 2019. Enzymatic modifications of chitin, chitosan, and chitooligosaccharides. Front. Bioeng. Biotechnol. 7, 1–26.
Kumar, M.N.R., 2000. A review of chitin and chitosan applications. React. Funct. Polym. 46 (1), 1–27.
Kurita, K., 1998. Chemistry and application of chitin and chitosan. Polym. Degrad. Stab. 59 (1–3), 117–120.
Li, M., Xia, J., Ding, C., Mao, W., Ding, H., Xu, L., Li, S., 2017. Development and characterization of ricinoleic acid-based sulfhydryl thiol and ethyl cellulose blended membranes. Carbohydr. Polym. 175, 131–140.
Min, B.M., Lee, S.W., Lim, J.N., You, Y., Lee, T.S., Kang, P.H., Park, W.H., 2004. Chitin and chitosan nanofibers: electrospinning of chitin and deacetylated of chitin nanofibers. Polymer 45, 7137–7142.
Noskov, S.Y., Lamoureux, G., Roux, B., 2005. Molecular dynamics study of hydration in ethanol–water mixtures using a polarizable force field. J. Phys. Chem. B 109 (14), 6705–6713.
Park, H.M., Misra, M., Drzal, L.T., Mohanty, A.K., 2004. "Green" nanocomposites from cellulose acetate bioplastic and clay: effect of eco-friendly triethyl citrate plasticizer. Biomacromolecules 5 (6), 2281–2288.
Pillai, C.K.S., Paul, W., Sharma, C.P., 2009. Chitin and chitosan polymers: chemistry, solubility and fiber formation. Prog. Polym. Sci. 34 (7), 641–678.
Poirier, M., Charlet, G., 2002. Chitin fractionation and characterization in N, N-dimethylacetamide/lithium chloride solvent system. Carbohydr. Polym. 50 (4), 363–370.
Qin, Y., Lu, X., Sun, N., Rogers, R.D., 2010. Dissolution or extraction of crustacean shells using ionic liquids to obtain high molecular weight purified chitin and direct production of chitin films and fibers. Green Chem. 12 (6), 968–971.
Rinaudo, M., 2006. Chitin and chitosan: properties and applications. Prog. Poly. Sci. 31 (7), 603–632.
Skołucka-Szary, K., Ramięga, A., Piaskowska, W., Janicki, B., Grala, M., Rieske, P., Bartczak, Z., Piaskowski, S., 2016. Synthesis and physicochemical characterization of chitin dihexanoate—a new biocompatible chitin derivative—in comparison to chitin dibutyrate. Mater. Sci. Eng. C 60, 489–502.
Sugimoto, M., Kawahara, M., Teramoto, Y., Nishio, Y., 2010. Synthesis of acyl chitin derivatives and miscibility characterization of their blends with poly

(ε-caprolactone). Carbohydr. Polym. 79 (4), 948–954.
Szosland, L., 1996. Synthesis of highly substituted butyryl chitin in the presence of perchloric acid. J. Bioact. Compat Polym. 11 (1), 61–71.
Teramoto, Y., Miyata, T., Nishio, Y., 2006. Dual mesomorphic assemblage of chitin normal acylates and rapid enthalpy relaxation of their side chains. Biomacromolecules 7 (1), 190–198.
Toivonen, M.S., Onelli, O.D., Jacucci, G., Lovikka, V., Rojas, O.J., Ikkala, O., Vignolini, S., 2018. Anomalous-diffusion-assisted Brightness in white cellulose nanofibril membranes. Adv. Mater. 30 (16), 1704050.
Van Luyen, D., Rossbach, V., 1995. Mixed esters of chitin. J. Appl. Polym. Sci. 55 (5), 679–685.
Wang, Y., Padua, G.W., 2010. Formation of zein microphase in ethanol-water. Langmuir 26 (15), 12897–12901.
Yang, B.Y., Ding, Q., Montgomery, R., 2009. Preparation and physical properties of chitin fatty acids esters. Carbohydr. Res. 344 (3), 336–342.
Yan, N., Chen, X., 2015. Sustainability: don't waste seafood waste. Nat. News 524 (7564), 155–157.
Zhang, Q., Hoogenboom, R., 2015. Polymers with upper critical solution temperature behavior in alcohol/water solvent mixtures. Prog. Polym. Sci. 48, 122–142.
Zhang, Q., Schattling, P., Theato, P., Hoogenboom, R., 2012. Tuning the upper critical solution temperature behavior of poly (methyl methacrylate) in aqueous ethanol by modification of an activated ester comonomer. Polym. Chem. 3 (6), 1418–1426.
Zhang, Y., Xue, C., Xue, Y., Gao, R., Zhang, X., 2005. Determination of the degree of deacetylation of chitin and chitosan by X-ray powder diffraction. Carbohydr. Res. 340 (11), 1914–1917.